(para), 127.4 and 125.7 (ortho and para), 55.3 ($N(CH_3)_4^+$), 53.6 ($CO\text{-}CH_3$).

$N(CH_3)_4^+$[*fac*-$(CO)_3(^{13}CO)Re(COCH_3)(COC_6H_5)]^-$ (5C). A solution of a 2:1 mixture (0.90 g, 1.83 mmol) of $N(CH_3)_4^+[(CO)_4Re(CH_3)(COC_6H_5)]^-$ (**7**): $N(CH_3)_4^+[(CO)_4Re(C_6H_5)(COCH_3)]^-$ (**6**) in 10 mL of acetone was placed in a 22-mL stainless steel Parr bomb and degassed by three freeze–pump–thaw cycles on a vacuum line. ^{13}CO (90% ^{13}C, Mound Laboratory) was condensed into the bomb at −196 °C. The bomb was sealed and warmed to 30 °C, where the gauge pressure was 400 psi. After 2 h at 30 °C, the ^{13}CO was vented and recovered for further use.

^1H NMR of the crude reaction mixture indicated that it consisted of 59% **5** in addition to 4% unreacted **7** and 37% unreacted **6**. The mixture was reacted with HCl (0.8 mL, 4.2 M in ether, 3.4 mmol) to convert **5C** to **10C**, which was isolated by column chromatography as for **10A**. Purified **10C** (0.44 g, 0.98 mmol) was then treated with $N(CH_3)_4^+OH^-$ (0.4 mL, 2.76 M in CH_3OH, 1.1 mmol) to give pure **5C** (0.24 g, 38% yield based on **7**): ^1H NMR (acetone-d_6, 270 MHz) δ 7.44 (m, 2 H), 7.23 (m, 3 H), 3.40 (m, 12 H), 2.25 (s, 3 H). ^{13}C NMR (acetone-d_6, 0.09 M $Cr(acac)_3$, −30 °C, 50.1 MHz) δ 262.9 (COC_6H_5), 260.5 ($COCH_3$), 196.1 (CO trans to $COCH_3$), 194.2 (CO's cis to both acyl groups, ~90× enhanced), 157.0 (ipso), 128.5 (para), 127.3 and 125.5 (ortho and meta), 55.1 ($N(CH_3)_4^+$), 53.4 ($COCH_3$), a peak expected at 195.0 due to CO trans to COC_6H_5 was not observed due to the proximity of the intense peak at 194.2; IR (Nujol) 2070 (sh), 2060 (m), 2045 (m), 1970 (s), 1955 (sh), 1942 (s), 1920 (s), 1903 (s), 1560 (m), 1535 (m) cm^{-1}.

***cis*-$(CO)_4(^{13}CO)ReC_6H_5$.** A solution of $(CO)_5Re^{13}COC_6H_5$ (2.0 g, 4.63 mmol) in 75 mL of acetone was heated at 96 °C for 1.8 h in a sealed Fischer–Porter bottle. Solvent was evaporated, and the residue was chromatographed (silica gel, hexane) to give *cis*-$(CO)_4(^{13}CO)ReC_6H_5$ (1.65 g, 88% yield): ^1H NMR (acetone-d_6, 270 MHz) δ 7.5 (m, 2 H), 7.0 (m, 3 H); ^{13}C NMR (acetone-d_6, 0.09 M $Cr(acac)_3$, −30 °C, 50.1 MHz) δ 185.1 (cis CO's, ~90× enhanced), 183.7 (s, trans CO), 145.9 and 129.0 (ortho and meta), 135.8 and 124.5 (ipso and para).

Reaction of *cis*-$(CO)_4(^{13}CO)ReC_6H_5$ with CH_3Li. CH_3Li (12 mL, 0.9 M, 10.8 mmol) was added to a solution of *cis*-$(CO)_4(^{13}CO)ReC_6H_5$ (2.25 g, 5.5 mmol) in 30 mL of THF at −78 °C. The solution was stirred for 1 h at −78 °C and warmed to room temperature. Several milliliters of H_2O were added to quench excess CH_3Li, and the solvent was evaporated under vacuum. An aqueous solution of $N(CH_3)_4^+Cl^-$ (25 mL, 1 M, 25 mmol) and 25 mL of CH_2Cl_2 was added to the residue. The CH_2Cl_2 layer was separated, and solvent was removed under vacuum. The residue was dissolved in THF and filtered. THF was removed under vacuum, and the resulting yellow solid was washed with ether and dried under vacuum to give $N(CH_3)_4^+[(CO)_4Re(C_6H_5)COCH_3]^-$ (**6**, 1.47 g, 54% yield): ^1H NMR (acetone-d_6, 200 MHz) δ 7.78 (m, 2 H), 6.77 (m, 3 H), 3.36 (s, 12 H), 2.23 (s, 3 H). In the ^{13}C NMR (acetone-d_6, 0.09 M $Cr(acac)_3$, −30 °C, 50.1 MHz), three major peaks were observed in a 1:2:1 ratio at δ 263.6 ($COCH_3$), 196.1 (CO's cis to both acyl groups), 195.4 (CO trans to $COCH_3$). In the ^{13}C NMR spectrum of a 1:4.3 mixture of this material and unlabeled **6**, an additional peak appeared at δ 195.6 (CO trans to C_6H_5), which was approximately $^1/_3$ the magnitude of the peak at 195.4.

Decarbonylation of 5. Acetone-d_6 solutions of **5**, **5A**, **5B**, and **5C** (~0.4 M) that also contained 0.09 M $Cr(acac)_3$ were heated at 68.5 ± 0.2 °C in an oil bath and monitored by ^{13}C NMR at 1, 5, 16, and 38 h. Details of ^{13}C NMR spectra are presented in the Results section.

^{13}C NMR. ^{13}C NMR spectra were obtained on a JEOL FX-200 spectrometer operating at 50.10 MHz. Spectra of ~0.4 M solutions of rhenium compounds were taken in acetone-d_6 containing $Cr(acac)_3$. Chemical shifts were measured relative to the acetone carbonyl resonance at δ 206.0. The samples were prepared by vacuum transfer of acetone-d_6 into 5-mm NMR tubes containing the rhenium compound and $Cr(acac)_3$ and were sealed under vacuum. All spectra were taken at −30 °C to reduce quadrupolar broadening due to rhenium. Experimental parameters used during data acquisition included a 90° pulse angle, 1.5-s delay between pulses, and broad-band proton decoupling. Integration of the spectra of ^{13}C natural abundance samples of **5**–**7** were in agreement (±10%) with expected peak ratios. Estimation of relative peak areas for overlapping peaks was made by comparison of observed spectra with computer-simulated spectra calculated as a sum of Lorentzian peaks. The rate of decarbonylation of labeled **5** in the presence of $Cr(acac)_3$ as measured by ^{13}C NMR was within experimental error of the decarbonylation rate in the absence of $Cr(acac)_3$ as measured by ^1H NMR.

Acknowledgment. Support from the National Science Foundation is gratefully acknowledged.

Registry No. **5**, 65583-15-5; **5A**, 83207-73-2; **5B**, 83207-75-4; **5C**, 83207-77-6; **6**, 65583-15-5; **6A**, 83207-79-8; **6C**, 83207-81-2; **6TA**, 83247-86-3; **6TP**, 83247-88-5; **7**, 65583-19-9; **10A**, 83214-24-8; **10B**, 83207-82-3; **10C**, 83207-83-4; $(CO)_5Re^{13}CoCH_3$, 83207-84-5; $(CO)_5Re^{13}COC_6H_5$, 83214-26-0; *cis*-$(CO)_4(^{13}CO)ReC_6H_5$, 83207-85-6; $CH_3{}^{13}COCl$, 1520-57-6; C_6H_5Li, 591-51-5; CH_3Li, 917-54-4; ^{13}CO, 1641-69-6; $C_6H_5{}^{13}COCl$, 52947-05-4; $NaRe(CO)_5$, 33634-75-2; $(CO)_5ReCOC_6H_5$, 56650-82-9; $(CO)_5ReC_6H_5$, 23625-72-1.

Crytalline-State Reaction of Cobaloxime Complexes by X-ray Exposure. 2. An Order-to-Order Racemization in the Crystal of [(*S*)-1-Cyanoethyl](pyridine)-bis(dimethylglyoximato)cobalt(III)

Yuji Ohashi,*[1a] Kazunori Yanagi,[1a] Toshiharu Kurihara,[1a] Yoshio Sasada,[1a] and Yoshiaki Ohgo[1b]

Contribution from the Laboratory of Chemistry for Natural Products, Tokyo Institute of Technology, Nagatsuta, Midori-ku, Yokohama 227, Japan, and Niigata College of Pharmacy, 5829 Kamishinei-cho, Niigata 950-21, Japan. *Received March 1, 1982*

Abstract: Crystals of [(*S*)-1-cyanoethyl](pyridine)bis(dimethylglyoximato)cobalt(III) undergo racemization in the crystalline state on exposure to X-rays. The reaction follows approximate first-order kinetics. The rate constants are 2.83×10^{-6} s^{-1} at 293 K and 5.06×10^{-5} s^{-1} in the early stages at 353 K. The crystal contains two crystallographically independent molecules in the $P2_1$ cell that are related by a pseudoinversion. On exposure to X-rays, the cyanoethyl group in one of the molecules in the asymmetric unit changes its configuration so that a crystallographic inversion center appears. The space group of the crystal becomes $P2_1/n$, and the volume of the unit cell decreases. The methyl group of the reacting cyanoethyl group makes unusually short contacts with a neighboring molecule in the initial stage. The steric repulsion from such short contacts is probably a driving force for the racemization of the crystal on X-ray exposure.

In a previous paper[2] we described the crystalline-state reaction of [(*R*)-1-cyanoethyl][(*S*)-α-methylbenzylamine]bis(dimethylglyoximato)cobalt(III) (**1**; hereafter bis(dimethylglyoximato)cobalt and the complex are abbreviated to cobaloxime and the *R*–*S* cyano

0002-7863/82/1504-6353$01.25/0

complex, respectively), where the racemization of the cyanoethyl

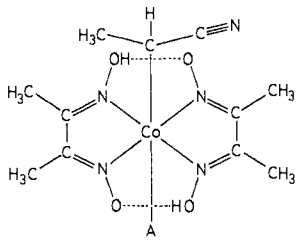

1, A = (*S*)-$NH_2CH(CH_3)C_6H_5$ [(*R*)-1-cyanoethyl]
2, A = (*S*)-$NH_2CH(CH_3)C_6H_5$ [(*S*)-1-cyanoethyl]
3, A = C_5H_5N [(*S*)-1-cyanoethyl]

group takes place without degradation of the crystallinity. The ordered enantiomer of the cyanoethyl group is converted into the disordered racemates. A similar order-to-disorder racemization was observed for the crystal of its diastereomer complex[3] (**2**, the *S*–*S* cyano complex). Because both complexes have a chiral amine, the noncentrosymmetric space group ($P2_1$) was preserved after the racemization of the cyanoethyl group. It seemed to be interesting to see whether or not the crystal chirality would be kept if the chiral amine was replaced with an achiral one. Several complexes containing achiral amines as the axial ligand were prepared. The crystal of [(*S*)-1-cyanoethyl](pyridine)cobaloxime (**3**) also revealed the crystalline-state racemization. The crystal chirality was not preserved after the racemization; that is, the space group was converted from a noncentrosymmetric to centrosymmetric one. The present paper reports this new type of crystalline-state reaction with a discussion of the mechanism of the reaction.

Experimental Section

The title complex was prepared by the method reported previously.[4] The orange platelike crystals were grown from an aqueous methanol solution. Preliminary determinations of the unit cell dimensions and space group were made from photographs. A crystal of 0.4 × 0.3 × 0.2 mm was mounted on a Rigaku four-circle diffractometer. Mo Kα radiation monochromated by graphite was used (50 kV, 30 mA, λ = 0.71069 Å). The determination of the cell dimensions using the least-squares technique with 15 reflections in the range of $20° < 2\theta < 30°$ was repeated continously in the early stages. The exposure time was recorded by a clock when the X-ray window-shutter was open. About 30 min was necessary for one cycle of the determination of the accurate cell dimensions. After 1 week, the change of the cell dimensions was monitored once a day. Figure 1 shows the changes of *a*, *b*, *c*, β, and *V* with changes in exposure time. The changes were within the experimental error after 20 days. The peak and integrated intensities decreased in the early stages, and then they recovered as observed for the *R*–*S* cyano crystal.[2] Crystal data for the initial and final stages are listed in Table I.

The three-dimensional intensity data were collected at the initial (I), intermediate (M), and final (F) stages by using a crystal of 0.5 × 0.4 × 0.2 mm. Each stage is indicated in Figure 1. In the course of the data collection, the orientation matrix was redetermined if the intensities of the three monitor reflections were significantly (greater than 6σ) changed. Reflections in the range of $3° \le 2\theta \le 50°$ were measured by an $\omega/2\theta$ scan, a scanning rate of 8°(2θ) min^{-1}, and a scan range of (1.0 + 0.35 tan θ)°. Stationary background counts were accumulated for 5 s before and after each scan. The reflections with $|F_o| \gtrsim 3\sigma(|F_o|)$ were used for the structure determination. The numbers of the independent reflections observed were 3406, 3170, and 2964 and the I, M, and F stages. No corrections for the absorption and extinction were made.

The intensities of *h*0*l* reflections with $h + l$ odd decreased significantly during the data collection and became negligibly small at the final stage. Table II shows the intensity changes of the several strong reflections with such indexes. The change indicates that the space group of the crystal is converted from the noncentrosymmetric $P2_1$ to the centrosymmetric $P2_1/n$.

The structure at the initial stage (I) was solved by the direct method with the MULTAN 78 program[5] and refined by the constrained least-

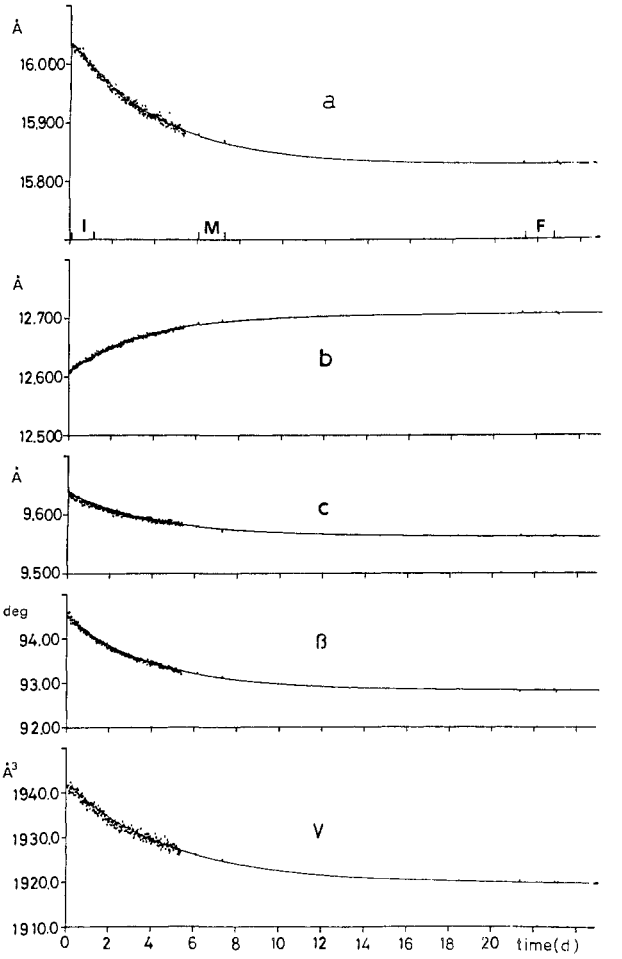

Figure 1. Change in the unit cell dimensions. First-order reaction curves are obtained by least-squares fitting using the observed values. Three-dimensional intensity data are collected at the three stages denoted as I (initial), M (intermediate), and F (final).

Table I. Crystal Data at the Initial and Final Stages

	initial	final
formula	$C_{16}H_{23}N_6O_4Co$	
M_r	422.33	
a, Å	16.036 (3)	15.824 (3)
b, Å	12.606 (1)	12.704 (1)
c, Å	9.634 (1)	9.559 (1)
β, deg	94.44 (2)	92.78 (2)
V, Å³	1941.7 (5)	1919.4 (5)
space group	$P2_1$	$P2_1/n$
Z	4	4
D_m, g cm^{-3}	1.445	
D_c, g cm^{-3}	1.445	
μ(Mo Kα), cm^{-1}	8.60	

Table II. Change of Intensities of Several *h*0*l* Reflections with $h + l$ = Odd

h	0	*l*	I[a]	M[b]	F[c]
−8	0	1	31.0 (2)	10.8 (4)	3.2 (8)
−4	0	3	34.1 (2)	11.8 (4)	3.8 (12)
−2	0	3	33.9 (2)	11.2 (4)	0.0 (8)
−13	0	4	40.9 (4)	12.8 (7)	7.5 (9)
−11	0	4	34.9 (3)	12.7 (6)	5.6 (8)

[a] Initial. [b] Intermediate. [c] Final.

(1) (a) Tokyo Institute of Technology. (b) Niigata College of Pharmacy.
(2) Ohashi, Y.; Yanagi, K.; Kuihara, T.; Sasada, Y.; Ohgo, Y. *J. Am. Chem. Soc.* **1981**, *103*, 5805–5812.
(3) Ohashi, Y.; Sasada, Y.; Ohgo, Y. *Chem. Lett.* **1978**, 743–746.
(4) Ohgo, Y.; Takeuchi, S.; Natori, Y.; Yoshimura, J.; Ohashi, Y.; Sasada, Y. *Bull. Chem. Soc. Jpn.* **1981**, *54*, 3095–3099.

Table III. Atomic Coordinates for the Initial Stage

atom	x/a	y/b	z/c	B_{eq},[a] Å^2
Co(A)	0.47956 (5)	−0.08578	0.26389 (8)	2.6
N(1A)	0.4611 (3)	−0.0914 (5)	0.4563 (5)	3.2
N(2A)	0.3880 (3)	−0.1817 (4)	0.2535 (6)	2.8
N(3A)	0.4977 (3)	−0.0789 (5)	0.0720 (5)	3.3
N(4A)	0.5749 (3)	0.0046 (4)	0.2731 (6)	3.1
O(1A)	0.5068 (3)	−0.0366 (4)	0.5567 (4)	3.8
O(2A)	0.3575 (3)	−0.2266 (4)	0.1353 (5)	3.7
O(3A)	0.4506 (4)	−0.1341 (4)	−0.0228 (5)	4.3
O(4A)	0.6076 (3)	0.0430 (4)	0.3948 (5)	3.6
C(1A)	0.4014 (4)	−0.1529 (5)	0.4907 (8)	3.5
C(2A)	0.3585 (4)	−0.2080 (5)	0.3713 (7)	3.1
C(3A)	0.5627 (4)	−0.0292 (6)	0.0391 (6)	3.2
C(4A)	0.6082 (4)	0.0219 (5)	0.1600 (7)	3.3
C(5A)	0.3771 (5)	−0.1695 (6)	0.6352 (7)	4.4
C(6A)	0.2896 (4)	−0.2857 (6)	0.3840 (8)	4.5
C(7A)	0.5906 (6)	−0.0267 (8)	−0.1073 (8)	5.9
C(8A)	0.6840 (4)	0.0919 (7)	0.1492 (9)	4.5
N(5A)	0.5592 (3)	−0.2116 (4)	0.2896 (5)	2.9
C(9A)	0.6130 (4)	−0.2213 (6)	0.4042 (7)	3.6
C(10A)	0.6687 (4)	−0.3026 (6)	0.4251 (7)	4.0
C(11A)	0.6684 (5)	−0.3821 (7)	0.3305 (9)	4.9
C(12A)	0.6132 (6)	−0.3773 (7)	0.2110 (9)	5.9
C(13A)	0.5589 (5)	−0.2908 (7)	0.1965 (7)	4.5
C(14A)	0.3995 (4)	0.0426 (5)	0.2508 (7)	3.4
C(15A)	0.3361 (4)	0.0254 (5)	0.1400 (7)	3.2
N(6A)	0.2848 (4)	0.0164 (6)	0.0452 (8)	5.5
C(16A)	0.4381 (5)	0.1500 (5)	0.2386 (9)	4.6
Co(B)	0.00860 (5)	0.08500 (8)	0.25130 (8)	3.0
N(1B)	0.0283 (3)	0.0925 (5)	0.0592 (5)	3.3
N(2B)	0.1036 (3)	0.1749 (4)	0.2614 (6)	3.7
N(3B)	−0.0095 (4)	0.0815 (5)	0.4415 (5)	4.0
N(4B)	−0.0856 (3)	−0.0032 (4)	0.2393 (6)	3.4
O(1B)	−0.0193 (4)	0.0383 (4)	−0.0383 (5)	4.5
O(2B)	0.1362 (3)	0.2155 (4)	0.3850 (5)	4.2
O(3B)	0.0388 (3)	0.1330 (4)	0.5424 (5)	4.5
O(4B)	−0.1179 (3)	−0.0459 (4)	0.1183 (5)	4.3
C(1B)	0.0887 (4)	0.1518 (6)	0.0235 (6)	3.5
C(2B)	0.1328 (4)	0.2028 (5)	0.1476 (8)	3.6
C(3B)	−0.0746 (4)	0.0267 (6)	0.4761 (7)	3.8
C(4B)	−0.1190 (4)	−0.0248 (6)	0.3573 (8)	3.8
C(5B)	0.1113 (6)	0.1690 (7)	−0.1238 (8)	5.4
C(6B)	0.2049 (5)	0.2785 (6)	0.1384 (10)	5.4
C(7B)	−0.1014 (5)	0.0200 (7)	0.6183 (8)	5.2
C(8B)	−0.1934 (4)	−0.0926 (7)	0.3701 (8)	5.0
N(5B)	−0.0677 (3)	0.2145 (4)	0.2260 (5)	2.9
C(9B)	−0.1296 (4)	0.2171 (5)	0.1268 (7)	3.5
C(10B)	−0.1829 (4)	0.3048 (6)	0.1089 (8)	4.5
C(11B)	−0.1727 (5)	0.3899 (6)	0.1962 (8)	4.1
C(12B)	−0.1080 (5)	0.3874 (6)	0.2990 (8)	4.9
C(13B)	−0.0587 (5)	0.2985 (6)	0.3123 (8)	4.3
C(14B)	0.0774 (6)	−0.0486 (7)	0.2873 (10)	5.4
C(15B)	0.1566 (5)	−0.0285 (6)	0.3652 (7)	4.2
N(6B)	0.2189 (4)	−0.0143 (6)	0.4282 (6)	4.8
C(16B)	0.0863 (7)	−0.1209 (9)	0.1713 (11)	8.0

[a] B_{eq} means the equivalent isotropic temperature factor.

squares method with the SHELX 76 program[6] in order to avoid parameter interaction between the two crystallographically independent molecules. The final refinement was carried out in the following manner: the non-hydrogen atoms were refined anisotropically, the C–CH_3 distances of the two cyanoethyl groups were constrained loosely to be 1.50 Å, and the hydrogen atoms were refined with fixed isotropic temperature factor (B = 8.0 Å^2). The weighting scheme of $w = (\sigma(|F_o|)^2 + 0.001338\ F_o^2)^{-1}$ was employed. Reflection 200 was not included in the final refinement because it suffered from the secondary extinction. No peaks higher than 0.5 e Å^{-3} were found in the final difference map. The final R value became 0.047 for 3405 reflections. The average cell dimensions before and after the data collection were used throughout the structure determination. They are a = 16.021 Å, b = 12.620 Å, c = 9.627 Å, and β = 94.27°. Atomic scattering factors were taken from ref 7.

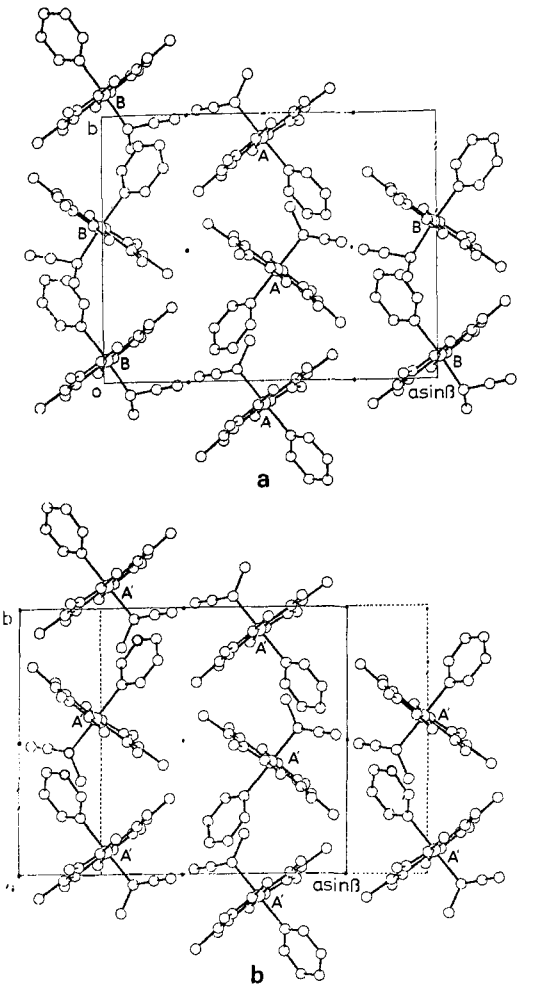

Figure 2. (a) Crystal structure at the initial stage (I) viewed along the c axis. Two crystallographically independent molecules A and B are related by a pseudoinversion indicated by a black circle. (b) Crystal structure at the final stage (F) viewed along the c axis. The original unit cell is indicated by dotted lines.

The structure at the final stage (F) was solved by the direct method with the program MULTAN 78 and refined by block-diagonal least squares with the modified HBLS program. All the hydrogen atoms were obtained on a difference map. The final refinement was performed with anisotropic temperature factors for the non-hydrogen atoms and isotropic temperature factors for the hydrogen atoms. The weighting scheme of $w = (\sigma(|F_o|)^2 + 0.000225\ F_o^2)^{-1}$ was employed. Reflection 200 was also excluded in the refinement. No peaks higher than 0.6 e Å^{-3} were found in the final difference map. The final R value became 0.054 for 2963 reflections. Atomic coordinates of the non-hydrogen atoms for the initial and final stages are given in Tables III and IV.[8]

The structure at the intermediate (M) stage was constructed by assuming a 1:1 composition of the initial and final structures. The R value became 0.070 for the structure. No significant peak greater than 1.0 e Å^{-3} was found in the difference map. Further refinement was not attempted.

For the experiments at higher temperatures, the hot-air gas-flow method was applied. The change of the cell dimensions by X-rays was observed at 353 K. Experimental details were the same as those at 293 K.

Results and Discussion

Change of the Crystal Structure. Figure 2a shows the crystal structure at the initial stage (I) viewed along the c axis. The two crystallographically independent molecules, A and B, are related to each other by pseudoinversion symmetry. Only the methyl

(5) Main, P.; Lessinger, L.; Woolfson, M. M.; Germain, G.; Declercq, J. P. MULTAN 78 (A system of a computer programs for the automatic solution of crystal structure from X-ray diffraction data), University of York, England, and Lauvain, Belgium, 1978.

(6) Sheldrick, G. M. SHELX 76 (A program for crystal structure determination), University of Cambridge, England, 1976.

(7) "International Tables for X-ray Crystallography"; Kynoch Press: Birmingham, England 1974; Vol. IV, pp 72–150.

(8) See paragraph at end of paper regarding supplementary material.

Table IV. Atomic Coordinates for the Final Stage

atom	x/a	y/b	z/c	B_{eq},[a] Å^2
Co	0.26708 (3)	0.08523 (4)	0.48725 (5)	2.8
N(1)	0.2876 (2)	0.0921 (2)	0.2944 (3)	3.2
N(2)	0.3605 (2)	0.1783 (2)	0.4950 (3)	3.3
N(3)	0.2481 (2)	0.0785 (2)	0.6802 (3)	3.6
N(4)	0.1719 (2)	−0.0040 (2)	0.4784 (3)	3.0
O(1)	0.2412 (2)	0.0362 (2)	0.1962 (2)	4.1
O(2)	0.3921 (2)	0.2210 (2)	0.6159 (3)	4.3
O(3)	0.2966 (2)	0.1317 (2)	0.7773 (2)	4.5
O(4)	0.1394 (2)	−0.0436 (2)	0.3577 (2)	3.9
C(1)	0.3476 (2)	0.1525 (3)	0.2574 (4)	3.3
C(2)	0.3909 (2)	0.2055 (3)	0.3766 (4)	3.4
C(3)	0.1825 (2)	0.0269 (3)	0.7148 (4)	3.5
C(4)	0.1371 (2)	−0.0231 (3)	0.5964 (4)	3.4
C(5)	0.3725 (3)	0.1690 (3)	0.1112 (4)	4.7
C(6)	0.4602 (3)	0.2825 (3)	0.3633 (5)	5.1
C(7)	0.1540 (3)	0.0204 (4)	0.8609 (4)	5.6
C(8)	0.0614 (2)	−0.0905 (3)	0.6114 (4)	4.7
N(5)	0.1876 (2)	0.2118 (2)	0.4641 (3)	3.0
C(9)	0.1312 (2)	0.2193 (3)	0.3549 (4)	4.0
C(10)	0.0781 (2)	0.3035 (3)	0.3347 (4)	4.4
C(11)	0.0825 (3)	0.3845 (3)	0.4286 (4)	4.7
C(12)	0.1393 (3)	0.3793 (3)	0.5389 (4)	5.2
C(13)	0.1902 (3)	0.2923 (3)	0.5547 (4)	4.2
C(14)	0.3489 (2)	−0.0403 (3)	0.4977 (4)	4.2
C(15)	0.4131 (2)	−0.0252 (3)	0.6086 (4)	3.7
N(6)	1.0354 (2)	0.4836 (3)	0.8058 (4)	5.1
C(16)	0.1880 (3)	0.3514 (4)	−0.0001 (5)	6.1

[a] B_{eq} means the equivalent isotropic temperature factor.

Table V. Bond Distances of the A and B Molecules at the Initial Stage and the A′ Molecule at the Final Stage

	distance, Å		
bond	A	B	A′
Co-N(1)	1.899 (6)	1.902 (6)	1.889 (3)
Co-N(2)	1.898 (5)	1.896 (6)	1.892 (3)
Co-N(3)	1.893 (6)	1.876 (6)	1.885 (3)
Co-N(4)	1.903 (6)	1.872 (6)	1.884 (3)
Co-N(5)	2.040 (6)	2.045 (5)	2.047 (3)
Co-C(14)	2.065 (7)	2.030 (9)	2.053 (4)
N(1)-O(1)	1.358 (8)	1.351 (8)	1.363 (4)
N(1)-C(1)	1.294 (10)	1.291 (9)	1.284 (4)
N(2)-O(2)	1.331 (7)	1.363 (8)	1.350 (4)
N(2)-C(2)	1.304 (8)	1.273 (9)	1.298 (4)
N(3)-O(3)	1.335 (8)	1.361 (8)	1.356 (4)
N(3)-C(3)	1.277 (9)	1.315 (10)	1.284 (5)
N(4)-O(4)	1.338 (7)	1.350 (8)	1.338 (4)
N(4)-C(4)	1.268 (9)	1.320 (9)	1.301 (4)
C(1)-C(2)	1.470 (10)	1.488 (10)	1.464 (5)
C(1)-C(5)	1.487 (11)	1.504 (12)	1.485 (5)
C(2)-C(6)	1.488 (10)	1.506 (12)	1.479 (6)
C(3)-C(4)	1.474 (10)	1.454 (10)	1.456 (5)
C(3)-C(7)	1.510 (13)	1.467 (12)	1.490 (6)
C(4)-C(8)	1.511 (11)	1.480 (11)	1.486 (5)
N(5)-C(9)	1.354 (9)	1.325 (8)	1.343 (5)
N(5)-C(13)	1.343 (10)	1.348 (9)	1.339 (5)
C(9)-C(10)	1.365 (10)	1.401 (10)	1.369 (5)
C(10)-C(11)	1.355 (11)	1.366 (11)	1.365 (6)
C(11)-C(12)	1.399 (13)	1.379 (11)	1.353 (6)
C(12)-C(13)	1.396 (13)	1.372 (11)	1.372 (6)
C(14)-C(15)	1.433 (10)	1.447 (12)	1.444 (5)
C(14)-C(16)	1.499 (11)	1.458 (15)	1.495 (6)
C(15)-N(6)	1.187 (10)	1.142 (11)	1.133 (5)

groups of the cyanoethyl groups of the two molecules destroy the true inversion symmetry because both of the cyanoethyl groups have *S* configuration. The molecules are packed as columns along the *b* axis. Each column is made up of either A or B molecules.

Figure 2b shows the crystal structure at the final stage (F) viewed along the *c* axis. Only the methyl group of the B molecule changes its position drastically, and the cyanoethyl group of B is converted from the *S* configuration to *R*. The A molecule does not change its structure, and the *S* configuration of the cyanoethyl group is conserved. The pseudoinversion center of the initial cell is changed to the crystallographic inversion center, and the crystal is transformed from the ordered enantiomeric structure to the ordered racemic one. This is in marked contrast to the cases of the *R*–*S* and *S*–*S* cyano crystals, for which the transformation occurs from the ordered enantiomeric structure to the disordered racemic one.

Table VI. Bond Angles of the A and B Molecules at the Initial Stage and the A′ Molecule at the Final Stage

	angle, deg		
angle	A	B	A′
N(1)-Co-N(2)	81.5 (2)	80.2 (3)	80.7 (1)
N(1)-Co-N(3)	179.5 (3)	178.4 (3)	179.3 (1)
N(1)-Co-N(4)	99.2 (3)	99.3 (2)	99.1 (1)
N(1)-Co-N(5)	89.6 (2)	89.1 (2)	89.5 (1)
N(1)-Co-C(14)	87.0 (3)	94.6 (3)	86.9 (1)
N(2)-Co-N(3)	98.7 (3)	98.4 (3)	98.7 (1)
N(2)-Co-N(4)	177.2 (2)	179.4 (3)	178.3 (1)
N(2)-Co-N(5)	89.1 (2)	89.9 (2)	89.3 (1)
N(2)-Co-C(14)	91.3 (3)	93.7 (3)	89.6 (1)
N(3)-Co-N(4)	80.6 (3)	82.2 (3)	81.5 (1)
N(3)-Co-N(5)	90.8 (2)	90.1 (2)	90.9 (1)
N(3)-Co-C(14)	92.5 (3)	86.3 (3)	92.7 (1)
N(4)-Co-N(5)	88.2 (2)	89.8 (2)	89.0 (1)
N(4)-Co-C(14)	91.5 (3)	86.7 (3)	92.1 (1)
N(5)-Co-C(14)	176.5 (3)	175.2 (3)	176.4 (1)
Co-N(1)-O(1)	124.1 (4)	121.6 (4)	122.4 (2)
Co-N(1)-C(1)	116.4 (5)	118.1 (5)	117.4 (2)
O(1)-N(1)-C(1)	119.5 (6)	120.3 (6)	120.2 (3)
Co-N(2)-O(2)	123.3 (4)	121.6 (4)	122.7 (2)
Co-N(2)-C(2)	116.5 (4)	117.8 (5)	117.0 (2)
O(2)-N(2)-C(2)	120.0 (5)	120.4 (6)	120.1 (3)
Co-N(3)-O(3)	121.5 (5)	124.4 (5)	122.4 (2)
Co-N(3)-C(3)	116.9 (5)	116.3 (5)	116.3 (2)
O(3)-N(3)-C(3)	121.1 (6)	119.3 (6)	121.1 (3)
Co-N(4)-O(4)	121.3 (4)	123.1 (4)	122.5 (2)
Co-N(4)-C(4)	116.8 (5)	116.5 (5)	116.3 (2)
O(4)-N(4)-C(4)	121.8 (6)	120.4 (6)	121.1 (3)
N(1)-C(1)-C(2)	113.3 (6)	110.9 (6)	112.6 (3)
N(1)-C(1)-C(5)	125.0 (7)	124.9 (7)	125.2 (3)
C(2)-C(1)-C(5)	121.7 (6)	124.2 (7)	122.1 (3)
N(2)-C(2)-C(1)	112.3 (6)	112.9 (6)	112.2 (3)
N(2)-C(2)-C(6)	124.0 (6)	123.9 (7)	123.9 (3)
C(1)-C(2)-C(6)	123.7 (6)	123.2 (7)	123.9 (3)
N(3)-C(3)-C(4)	112.6 (6)	112.7 (6)	113.4 (3)
N(3)-C(3)-C(7)	123.1 (7)	124.0 (7)	123.6 (3)
C(4)-C(3)-C(7)	124.3 (7)	123.3 (7)	123.0 (3)
N(4)-C(4)-C(3)	112.8 (6)	112.3 (6)	112.3 (3)
N(4)-C(4)-C(8)	123.5 (6)	124.9 (7)	124.6 (3)
C(3)-C(4)-C(8)	123.6 (6)	122.8 (7)	123.1 (3)
Co-N(5)-C(9)	121.6 (5)	120.9 (4)	121.4 (2)
Co-N(5)-C(13)	121.8 (5)	121.3 (5)	122.0 (2)
C(9)-N(5)-C(13)	116.5 (6)	117.7 (6)	116.6 (3)
N(5)-C(9)-C(10)	123.9 (7)	121.7 (6)	123.0 (3)
C(9)-C(10)-C(11)	119.2 (7)	120.1 (7)	119.0 (4)
C(10)-C(11)-C(12)	119.5 (8)	118.2 (7)	119.1 (4)
C(11)-C(12)-C(13)	117.8 (9)	118.8 (7)	119.3 (4)
N(5)-C(13)-C(12)	123.0 (8)	123.5 (7)	123.0 (4)
Co-C(14)-C(15)	109.2 (5)	112.8 (6)	110.6 (3)
Co-C(14)-C(16)	117.1 (5)	118.2 (7)	118.0 (3)
C(15)-C(14)-C(16)	110.6 (6)	112.0 (8)	111.8 (4)
C(14)-C(15)-N(6)	176.3 (8)	178.7 (9)	177.7 (4)

The racemic crystals of the present complex were prepared from an aqueous methanol solution, although they were too small for structure determination. They have the same cell dimension and space group as the racemic crystal obtained by X-ray exposure.

Conformational Change of the Molecule. Bond distances and angles of the initial A and B and final A′ molecules are listed in Table V and VI, respectively. The corresponding values of the three molecules coincide with each other within experimental error and are in good agreement with those of the related compounds.[9,10]

(9) Ohashi, Y.; Sasada, Y.; Takeuchi, S.; Ohgo, Y. *Bull. Chem. Soc. Jpn.* **1980**, *53*, 627–634.

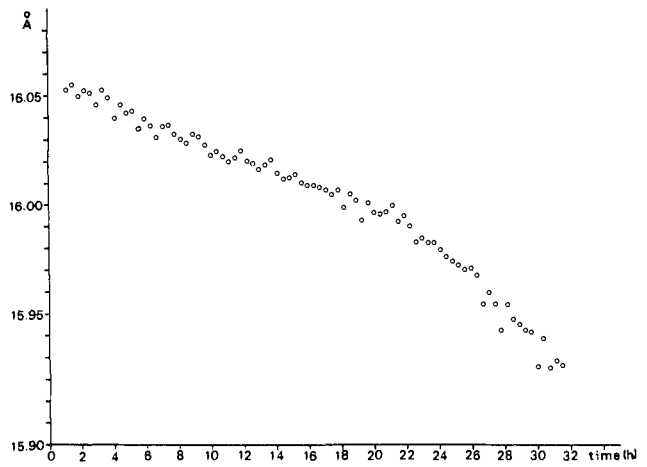

Figure 3. Change of a with the exposure time. First-order reaction curve in the early stages (before 16 h) fits the data well.

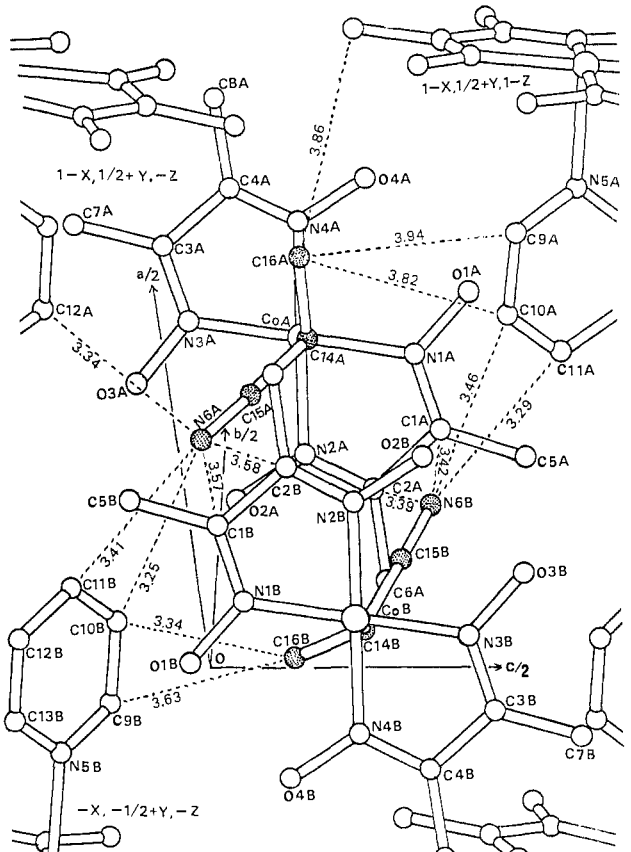

Figure 4. Neighborhood of the two cyanoethyl groups around the pseudoinversion center (initial stage) viewed along the normal to the A cobaloxime plane and the short interatomic distances. Shaded atoms are those of the cyanoethyl groups in the original unit. Coordinates indicate the equivalent positions.

On the other hand, the rotation angles around the Co–C and Co–N bonds are different for the three molecules. The torsional angles of C(15)–C(14)–Co–N(2) and C(9)–N(5)–Co–N(1) of the A, B, and A′ molecules are given in Table VII. When the crystal is racemized, the Co–C bond of B rotates by 21.7°, whereas that

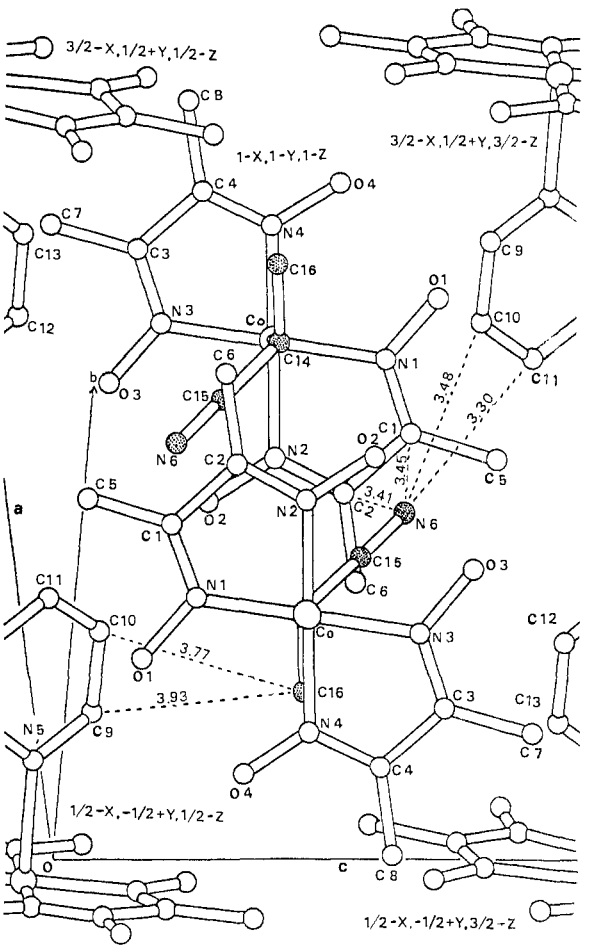

Figure 5. Neighborhood of the two cyanoethyl groups around the inversion center (final stage) viewed along the normal to the cobaloxime plane and the short interatomic distances. Shaded atoms correspond to those in Figure 4. Coordinates indicate the equivalent positions.

of A does only by 0.9°. Since the absolute configuration of the cyanoethyl group of B is inverted, the cyanoethyl group should rotate around the Co–C bond to avoid steric repulsion with the surrounding molecules. The torsional angles of C(9)–N(5)–Co–N(1) in A and B are different by 12.8°. After the racemization, they become 43.6°, which is close to the average, 45.8°, for the A and B molecules.

Rate of Racemization. Figure 1 clearly indicates that the racemization proceeds in first-order kinetics. The rate constants k_a, k_b, k_c, k_β, and k_v, were calculated to be 2.79×10^{-6}, 3.29×10^{-6}, 2.77×10^{-6}, 2.87×10^{-6}, and 2.41×10^{-6} s^{-1}, respectively. The theoretical curves are drawn in Figure 1. The average, 2.83×10^{-6} s^{-1}, is slightly smaller than the corresponding value, 3.06×10^{-6} s^{-1}, for the R–S cyano crystal.[2]

The change in the cell dimensions was measured at 353 K. The initial values of a, b, c, β, and V at 353 K are 16.063 (6) Å, 12.735 (2) Å, 9.666 (2) Å, 94.20 (3)°, and 1972.0 (9) Å^3, respectively. When the crystal was irradiated by X-rays at 353 K, the unit cell dimensions changed much faster than those at 293 K. Figure 3 shows the change of a with the change in exposure time. Changes of other dimensions were similar to a. The plot apparently indicates that in the early stages the reaction proceeds in first-order kinetics. The rate constant k_a was calculated to be 5.06×10^{-5} s^{-1}, which is about 18 times that at 293 K. After 16 h, however, the rate of change increased. The peak and integrated intensities gradully decreased, although they recovered after the early stages at 293 K. The rate of change became so fast that the crystal no longer remained in a single-crystal form. After 32 h, it was impossible to continue accurate determination of the cell dimensions. The values of a, b, c, β, and V were found to be 15.937 (7) Å, 12.783 (3) Å, 9.612 (3) Å, 93.02 (4)°, and 1955 (1) Å^3,

(10) Ohashi, Y.; Sasada, Y.; Takeuchi, S.; Ohgo, Y. *Bull. Chem. Soc. Jpn.* **1980**, *53*, 1501–1509.

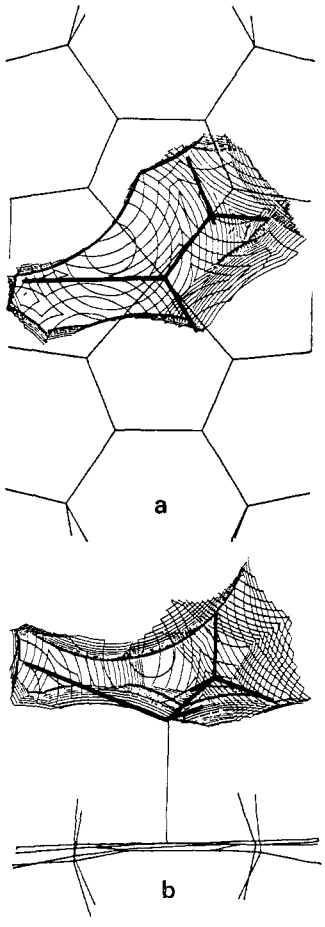

Figure 6. Cavity for the A cyanoethyl group viewed along (a) the normal to the cobaloxime plane and (b) the long axis of cobaloxime. Contours are drawn in sections separated by 0.1 Å.

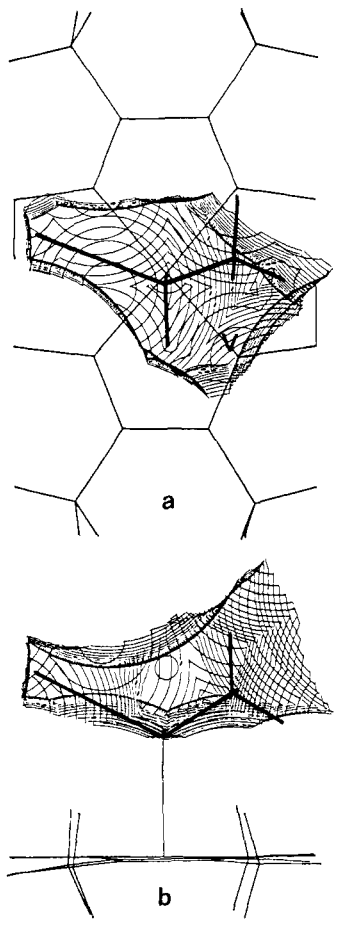

Figure 7. Cavity for the B cyanoethyl group drawn in the same way as in Figure 6. Void space is denoted as V.

respectively. When the temperature was lowered to 293 K, they were 15.86 (1) Å, 12.680 (5) Å, 9.571 (5) Å, 93.03 (7)°, and 1922 (2) Å^3, respectively, which are close to the corresponding final values listed in Table I, and they probably would have converged to the values of the racemic crystal if the high-temperature experiment could have been continued. Above 353 K, the crystal was decomposed by X-ray exposure.

In order to confirm whether or not the crystal was racemized without X-ray exposure at high temperatures, it was kept for a week at 353 ± 0.3 K in a dark thermostat. It had the same unit cell dimensions as before the experiment. The crystal is, therefore, racemized only by X-ray exposure.

Reaction Mechanism. Figure 4 shows the neighborhood of the two cyanoethyl groups around the pseudoinversion center together with short interatomic distances at the initial stage. The cyanoethyl group of the A molecule, the A cyanoethyl group, makes the usual van der Waals contacts with the surrounding molecules. The B cyanoethyl group, on the other hand, very closely approaches the neighboring molecules on the left side whereas it has loose contacts on the right side. The distance, 3.34 Å, between the methyl group, C (16B), and C(10B) of the pyridine ligand at $-x, -{}^1/_2 + y, -z$ is unusually short, but this great hindrance cannot be relieved by the rotation around the Co–C bond because N(6B) at the other end of the cyanoethyl group also makes a short contact with C(2A), 3.39 Å. This fact suggests that the inversion of the configuration of the B cyanoethyl group is energetically favorable. On the other hand, the A cyanoethyl group can have the opposite configuration only with difficulity since the methyl group, C(16A), has the usual van der Waals contacts with the neighboring pyridine ligand on the right side.

Figure 5 shows the same region at the final stage. When the B cyanoethyl group is changed from the *S* configuration to *R* by X-ray exposure, the unusually short contact between C(16B) and the pyridine ligand disappears and a wide void space remains at the original position of the methyl group. To fill up the void, the B cyanoethyl group rotates around the Co–C bond and the two molecules of A and B approach each other. Since the A and B molecules are in contact along the *a* axis (see Figure 2), the crystal contracts to a great extent along the *a* axis.

In order to examine the above discussion more quantitatively, we have defined the cavity for the cyanoethyl group as the concave space.[2] Any point in the cavity is then considered to be accessed by the centers of the atoms of the cyanoethyl group. Figure 6 shows the cavity for the A cyanoethyl group at the initial stage projected (a) along the normal to the cobaloxime plane and (b) along the long axis of the cobaloxime. The cyanoethyl group is well fitted in the cavity, and no void space is observed. Figure 7 shows the corresponding cavity for the B cyanoethyl group. The cavity does not fully accommodate the group; that is, two of the methyl hydrogen atoms protrude from the cavity. The methyl group must sustain the strong steric repulsion from the surrounding molecules. On the other hand, there is a void adjacent to the methyl group denoted as V.

Figure 8 shows the corresponding cavity for the A′ cyanoethyl group with the *R* configuration at the final stage. The A′ cyanoethyl group with the *S* configuration has, of course, the mirror image of the cavity in Figure 8. The shape of the cavity at the final stage is similar to that of the A cyanoethyl group. The two cavities of the cyanoethyl groups of B and A′ are compared in Figure 9. The side view is omitted since the two side views are nearly the same. If the B cyanoethyl group changes from the *S* configuration to *R*, it fits well in the final racemic cavity.

The volume of each cavity was calculated by the same method described previously.[2] The cavities of the A, B, and A′ cyanoethyl groups have volumes of 8.89, 11.34, and 10.52 Å^3, respectively. The cavity of the B cyanoethyl group is significantly larger than that of A and becomes smaller after the racemization.

Table VII. Torsional Angles of the Co–C and Co–N Bonds

molecule	angle, deg: C(15)–C(14)–Co–N(2)	angle, deg: C(9)–N(5)–Co–N(1)
A	46.9	39.4
B	26.1	52.2
A′	47.8	43.6

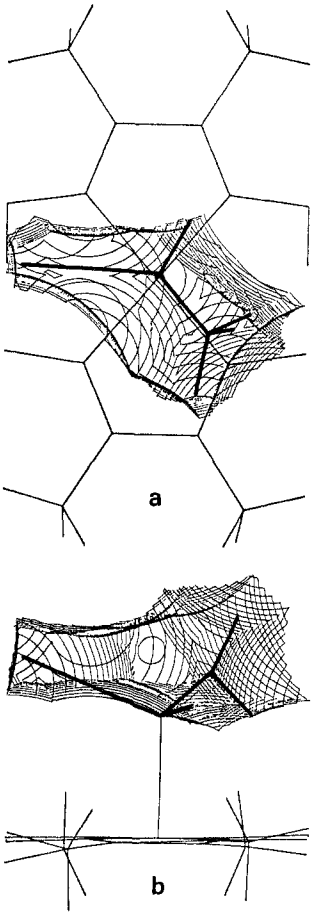

Figure 8. Cavity for the A′ cyanoethyl group with the *R* configuration drawn in the same way as Figure 6.

The cavity of the A cyanoethyl group is too compact to take the group with the opposite configuration. This brought about the idea that the A cyanoethyl group might also have the opposite configuration at high temperatures. The crystal was irradiated by X-rays at 353 K. This only increased the reaction rate of the crystal but did not induce inversion of the configuration of the A cyanoethyl group. Although the volume of the cavity at 353 K could not be obtained, the above results suggest that not only the volume but also the shape of the cavity is important for the inversion of the configuration of the cyanoethyl group.

In the *R–S* and *S–S* cyano crystals, no strong steric repulsions were found at the initial stage. When the racemization occurs by X-ray exposure, each cyanoethyl group has a disordered structure containing *R* and *S* configurations and the volume of the unit cell increases. The racemic structure would be more stable thermodynamically than the original one. The increasing entropy

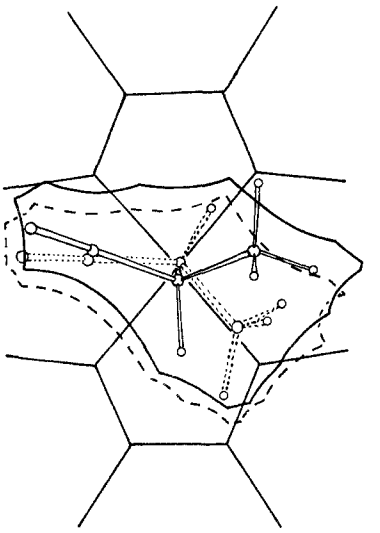

Figure 9. Comparison of the two cavities for the B (solid) and A′ (dotted) cyanoethyl groups. Solid and dotted curves indicate the peripheries of the cavities for the B and A′ cyanoethyl groups, respectively.

may cause the racemization of the cyanoethyl group. On the other hand, the methyl group of the B cyanoethyl group suffers from the fairly strong steric repulsion in the present crystal. A driving force for the racemization would be the steric repulsion. The final racemic structure is probably more favorable energetically than the initial one. Because of nearly identical cell dimensions and crystal structure of the enantiomer and racemate, a whole crystal is converted into the ordered racemic structure without destroying the single-crystal form.[11]

Acknowledgment. This work was partly supported by a Grant-in-Aid for Scientific Research from the Ministry of Education, Science and Culture, Japan. The high-temperature facility was partly supported by a Grant from RCA Research Laboratories, Inc.

Registry No. (*S*)-**3**, 83289-17-2; (*R*)-**3**, 80514-18-7.

Supplementary Material Available: Tables of the observed and calculated structure factors, anisotropic thermal parameters for non-hydrogen atoms, and the positional and isotropic thermal parameters at the initial and final stages (27 pages). Ordering information is given on any current masthead page.

(11) It has been extensively observed from ESR measurements that the Co–C bond in alkyl(pyridine)cobaloxime complexes is homolytically cleaved by visible light ($\lambda > 420$ nm) in solution (references are shown in ref 2). A similar ESR spectra was observed after the *R–S* crystal was irradiated by X-rays for 30 min.[2] However, when the aqueous methanol solution containing the *R–S* complex was exposed to X-rays and to visible light separately, the racemization by X-rays was much slower than that caused by visible light. Although the absolute intensities may be different between the X-rays and the visible light, this fact seems to indicate that the photons produced by the interaction between the X-rays and the crystal are responsible for the Co–C bond cleavage in the crystalline state. On exposure to X-rays, the appearance of the crystals showed no decomposition or degradation. Examination through a microscope with polarized light revealed no boundaries between the original and racemic phases in the crystal. The diffuse scattering due to long-range ordering was not found on Weissenberg photographs at the intermediate stages. When the crystal was exposed to room light for a long time, its surface was slightly decomposed but its cell dimensions were the same as those of the fresh crystals. These facts suggest that the X-rays introduce nucleation sites of the racemic phase at random inside the crystal and that such a random nucleation is essential for the maintenance of crystallographic ordering.